Available online at www.sciencedirect.com
ScienceDirect
Electrochimica Acta 53 (2007) 1417–1421
ELECTROCHIMICA Acta
www.elsevier.com/locate/electacta

Lithium ion conductivity of molecularly compatibilized chitosan–poly (aminopropyltriethoxysilane)–poly(ethylene oxide) nanocomposites

S. Fuentes [a], P.J. Retuert [b], G. González [c,*]

[a] Department of Physics, Faculty of Sciences, Universidad Católica del Norte, Angamos 0610, Antofagasta, Chile
[b] Department of Material Sciences, Faculty of Mathematical and Physical Sciences, Universidad de Chile, Tupper 2069, Santiago, Chile
[c] Department of Chemistry, Faculty of Sciences, Universidad de Chile, Casilla 653, Santiago, Chile

Received 26 December 2006; received in revised form 22 May 2007; accepted 23 May 2007
Available online 31 May 2007

Abstract

Films of composites of chitosan/poly(aminopropyltriethoxysilane)/poly(ethylene oxide) (CHI/pAPS/PEO) containing a fixed amount of lithium salt are studied. The ternary composition diagram of the composites, reporting information on the mechanic stability, the transparence and the electrical conductivity of the films, shows there is a window in which the molecular compatibility of the components is optimal. In this window, defined by the components ratios CHI/PEO 3:2, pAPS/PEO 2:3 and CHI/PEO 1:2, there is a particular composition $Li_x(CHI)_1(PEO)_2(pAPS)_{1.2}$ for which the conductivity reaches a value of 1.7×10^{-5} S cm^{-1} at near room temperature. Considering the balance between the Lewis acid and basic sites available in the component and the observed stoichiometry limits of formed polymer complexes, the conductivity values of these products may be understood by the formation of a layered structure in which the lithium ions, stabilized by the donors, poly(ethylene oxide) and/or poly(aminopropyltriethoxysilane), are intercalated in a chitosan matrix.

Keywords: Chitosan; Poly(ethylene oxide); Poly(aminopropyltriethoxysilane); Lithium ionic conductor; Polymer electrolyte

1. Introduction

Electrical conductivity as well as the mechanical and chemical stability are, in general, the most important properties of materials to be used as electrolytes in solid-state devices. However, depending on the type of applications, other properties have also to be considered. Thus, the flexibility needed for getting films useful in microdevices or the transparence in a given light frequency range required for electroptical applications may be also important in the development of new ion-conducting materials. Both, the adaptability to any type of spaces and the functional versatility of polymers make them especially suitable in the development of solid electrolytes [1–4]. Indeed, during the last decades, most efforts for obtaining new high efficient conducting polymer electrolytes have been focused on composites based on polyethers as poly(ethylene oxide) (PEO) and poly(propylene oxide) (PPO) [5,6]. Products containing the polymers and lithium salt as main components often lead to enough robust materials with conductivities of the order of 10^{-6} to 10^{-7} S cm^{-1} at room temperature. However, there are still some unresolved problems in the use of PEO-based systems. Most of them are related to the relatively high crystallinity degree that enhances the rigidity of the polymers at room temperature threading both the conductivity and the transparence of the products [7,8]. Acceptable improvements of the conductivity at low temperatures are afforded by the addition of low molecular electron pair donors, generally common organic solvents able to act as plasticizers that increases the solubility of inorganic salt solvating the lithium ion and enhances the flexibility of the polymer favoring the chain movement [9]. The use of plasticizers, limited only by the mechanical stability of the product, does not however guarantee the transparence of the composite, which is mostly determined by the chemical compatibility of the components.

Chitosan has an exceptional film-forming aptitude. Indeed, it has been widely used for coating purposes especially because of its capacity to form relatively robust films [10]. Optical transparence of chitosan is relatively poor. This

* Corresponding author.
E-mail address: ggonzale@uchile.cl (G. González).

0013-4686/$ – see front matter © 2007 Elsevier Ltd. All rights reserved.
doi:10.1016/j.electacta.2007.05.057

polymer generally shows high crystallinity leading to rather rigid and opaque films. However, the rich functionality of this polyaminosaccharide makes possible the formation of composites in which the molecular compatibility of the components leads to transparent products [11–14]. One example of that is the macromolecular complex formed by chitosan and poly(aminopropyltriethoxysilane) (pAPS) which leads to robust, flexible and transparent films [15]. The incorporation of lithium salts to these mixtures also leads to products with similar properties but they, however, behave as ionic conductors. Interestingly, the presence of lithium salts induces drastic changes in the structures of the nanocomposites often leading to layered structures which could be described as an intercalation compound in which lithium ions are located in the interlaminar spaces defined by a relatively more rigid polymer phase. From our experience on intercalation chemistry we know that in such structural arrangements lithium mobility often shows improved results [16,17].

Encouraged by both, the well-known ability of poly(ethylene oxide) for leading to good solid ionic conductors commented above and our experience of obtaining transparent materials based on chitosan nanocomposites, we decided to explore the ternary system chitosan/poly(aminopropyltriethoxysilane)/poly(ethylene oxide) containing a fixed amount of lithium salt. In this paper, the behavior of a series of these composites is described, analyzing principally the mechanic stability, the transparence and the electrical conductivity of their films.

2. Experimental

2.1. Reagents

Chitosan (CHI) (Bioquímica Austral Ltd., Chile) with an average molecular weight of 3.5×10^5, and a deacetylation degree of 87.5% was washed with acetone and methanol and dried to constant weight. CHI was used as 1% solutions in diluted formic acid (5%). 3-Aminopropyltriethoxysilane (APS) (Aldrich) was hydrolyzed in 0.5 M formic acid at 45 °C for 3 days leading to a solution containing 3-aminopropyltriethoxysilane oligomers (pAPS) with $M_w \sim 800$ as determined by size-exclusion chromatography (Bruker LC 21B equipped with a Shodex OH pack 803-column). The solution was used after partial solvent evaporation when its concentration was about 0.7 g pAPS/ml. Poly(ethylene oxide) (Aldrich, $M_w = 4 \times 10^6$) was dissolved in water.

2.2. Film preparation

PEO, CHI and pAPS solutions in the appropriate ratios were stirred for about 24 h at room temperature. Anhydrous lithium perchlorate (Merck) was added as a 1 M solution in absolute ethanol. Films of 0.07–1.5 mm thickness were prepared by solution casting on a Petri dish and then dried by evaporation at room temperature.

2.3. Film characterization

Products were characterized by differential thermal analysis, DSC (STA 625, Polymer Laboratories), X-ray diffraction analysis (Siemens D-500), scanning electron microscopy (Philips EM 300) and UV–vis spectroscopy (UV-2450 Shimadzu). Electrochemical impedance spectroscopy (PAR Model 6310 Electrochemical Impedance Analyzer) were performed under argon atmosphere in range from 100 mHz to 100 kHz using ion-blocking gold electrodes at 40 ± 0.2 °C.

3. Results and discussion

The properties of the products obtained by blending CHI, pAPS and PEO depend on the ratio of the components. The two ternary diagrams illustrated in Fig. 1 indicate the concentration ranges of the components for which mechanically stable self-supported films are obtained and the electrical conductivity of the films, respectively. The amount of chitosan appears to be determinant for the mechanic stability of the films. In the lower part of the diagram, dominated by the influence of pAPS, are grouped together, mixtures leading to viscous liquids or solids which do not permit the formation of transparent

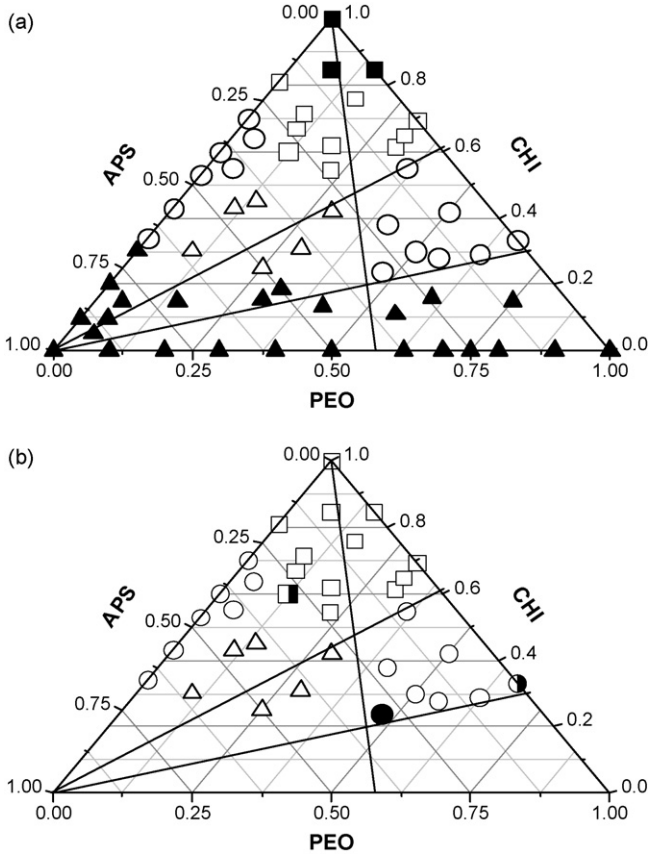

Fig. 1. PEO/CHI/pAPS ternary phase diagram. (a) Mechanical stability and transparence of films prepared in the presence of 0.2 M $LiClO_4$: no film formation (▲); brittle and opaque (△); transparent and flexible (◯); yellowish and flexible (□); flexible and opaque (■). (b) Electrical conductivity of self-supporting films observed in the ranges: $\leq 10^{-7}$ S cm^{-1} (◯, □ and △); 10^{-6} S cm^{-1} (◨ and ◑); 10^{-5} S cm^{-1} (●).

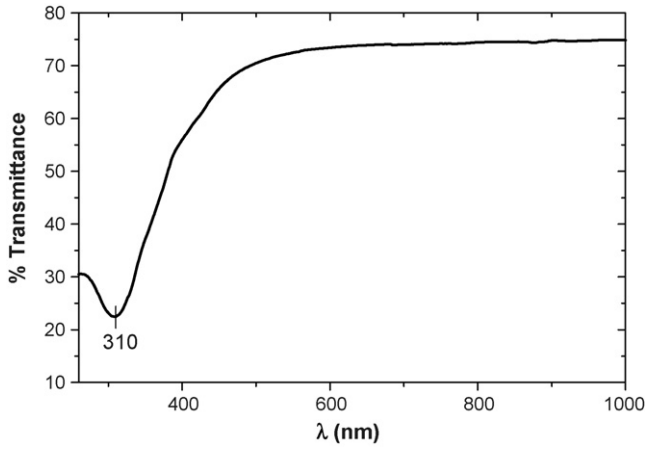

Fig. 2. UV–vis transmission spectrum of a 0.1 mm thick film of the nanocomposite POE/CHI/pAPS/Li^+ 1:0.5:0.6:0.2.

self-supported films. No appropriate binary PEO/pAPS materials were indeed obtained. Although binary mixtures of PEO and chitosan always lead to robust films, PEO-rich mixtures lead to brittle, yellowish, opaque materials. In the CHI/pAPS binary mixtures, the maximal amount of pAPS for obtaining workable films is about 64%. Conductivity also increases with increasing exchange of the polyether by pAPS around lithium in the mobile phase. pAPS appears thus having an effect on the ionic conductivity like that of the plasticizer in the conventional PEO-based polymer electrolytes.

From our point of view, the most important property of some of the composites obtained here is their transparence; so far it points to the molecular compatibility of the components, so the products may be considered as nanocomposites. In the ternary CHI/APS/PEO diagram illustrated in Fig. 1a it may be visualized the windows where transparent, flexible films are obtained. There are only two relatively narrow zones where binary CHI/pAPS mixtures containing a maximum of about 64% pAPS are transparent while the CHI/PEO ones meet that condition up to about 70% PEO. Ternary mixtures form transparent films in the composition window defined in approximately the ranges 40–70, 30–70 and 0–30% of CHI, PEO and pAPS, respectively.

The transparence of the film POE/CHI/pAPS/Li^+ 1:0.5:0.6:0.2 which is interesting due to its electrical conductivity (Fig. 1b) is illustrated in Fig. 2 which reports the transmission spectrum in the UV–vis range. The transmittance of the film reaches about 80% in the visible spectral range. The transmission spectrum of the film POE/CHI/Li^+ 1:0.5:0.2, for which also a rather acceptable conductivity was observed (see below), as well as that of the other films in the same transparence window, are similar to that illustrated in Fig. 2.

The typical electrical transport behavior of the films between ion-blocked gold electrodes reported in this work (Fig. 1b) may be visualized in the Nyquist diagram illustrated in Fig. 3 presenting the imaginary ($-iZ''$) against the real (Z') component of the impedance (Z) data. Most films show conductivities $\leq 10^{-7}$ S cm^{-1}; however, there are some compositions for which conductivity values of the order of 10^{-6} S cm^{-1} (◨ and ◑

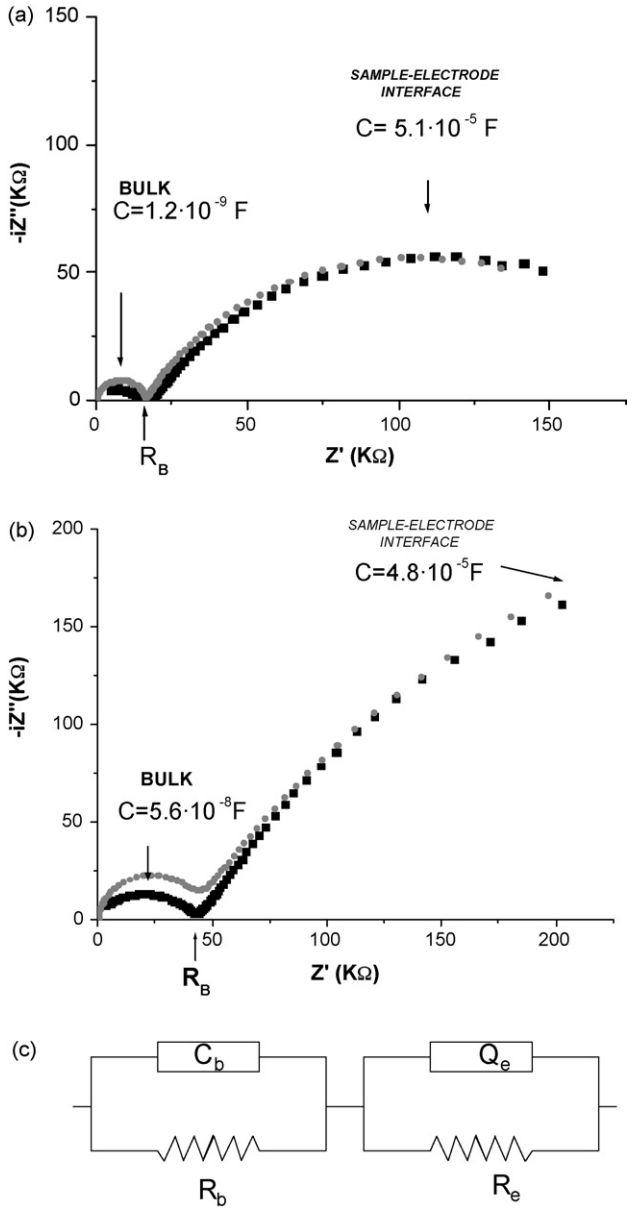

Fig. 3. Nyquist plots for the films. (a) POE/CHI/pAPS/Li^+ 1:0.5:0.6:0.2; (b) POE/CHI/Li^+ 1:0.5:0.2; (c) equivalent electrical circuit (R_bC_b) (R_eQ_e). Curves in gray correspond to simulations of proposed equivalent circuit using a CPE with $B = 4.9 \times 10^{-6}$ and $n = 0.71$ in (a) and $B = 5 \times 10^{-6}$ and $n = 0.68$ in (b), respectively.

in Fig. 1) are observed, namely the points with 6.6×10^{-6} and 1.2×10^{-6} S cm^{-1} and a very singular point of composition PEO/QO/pAPS/Li^+ 1:0.5:0.6:0.2 located in the window of the molecularly compatible ternary mixtures, where a maximal value of 1.7×10^{-5} S cm^{-1} (●) is reached. The analysis of the curves in Fig. 3 may be performed considering the observed capacitance (C) ranges. The capacitance in the first semicircle depends on the composition of the film, being about 10^{-8} and 10^{-9} F for films with and without pAPS, respectively. Such a process corresponds to the polarization of the electroactive species in the bulk of the sample, leading directly to the conductivity values analyzed above. After the first semicircle follows a second one whose capacitance value of about 10^{-5} F is

invariant to the composition of the sample. The latter may be ascribed to processes occurring in the interface sample–electrode which are determined by the polarization at the blocking electrodes [18]. Charge migration and polarization processes like those described by the Nyquist plots in Fig. 3 may often be associated to equivalent electrical circuits constituted by a resistor and a capacitor placed in parallel. In our case, this simple model may be indeed applied for representing the processes occurring in the bulk, (R_bC_b) in Fig. 3c.There, the capacitance contribution to the impedance is represented by the function $iZ'' = (C_b i\omega)^{-1}$, where $i = \sqrt{(-1)}$, ω the angular frequency and C_b is the bulk capacitance. However, to describe satisfactorily the experimental results arising from the polarization at an interface with a fractal or fractional dimension of roughness, as probably occurs because of the porosity observed in our films, a more complex model is needed. Therefore, for modeling the process occurring at the sample–electrode interface (R_eQ_e in Fig. 3c), we have considered an approach often used in solid-state electrochemistry consisting of a constant phase element (CPE), Q the universal capacitor where the capacitance contribution is represented by a fractional power law on the frequency: $iZ'' = B(i\omega)^{-n}$, being B the constant and n the parameter which varies between 0.5 and 1 [19].

The morphology of obtained films may be appreciated in the images reproduced in Fig. 4. It may be clearly appreciated that the structure of the films corresponds to a self-assembled layered arrangement with a considerable order degree. In the same figure, it is also to be observed that when the morphologies of films with the compositions PEO/CHI/pAPS/Li^+ 1:0.5:0.5:0.2 and PEO/CHI/Li^+ 1:0.5:0.2 are compared, those containing pAPS are notoriously more porous, a feature which is possibly related to the relative higher conductivity of these nanocomposites.

In spite of the lamellar structure and relatively high pAPS content, the nanocomposite with highest conductivity CHI/PEO/pAPS/Li^+ 0.5:1:0.6:0.2 has, as shown in Fig. 5, a thermal behavior like that of a compound with only one well-defined decomposition temperature. However, if we compare that temperature with the decomposition of the macromolecular complex CHI/pAPS 0.6:1, 360 °C [15] the effect of both, the lithium ion and the more flexible layer structure, may be appreciated.

Assuming that transparence is a criterion appropriate for discerning molecular compatibility, the window defined in the phase diagram described above (Fig. 1) should be explainable considering the molecular interactions being there among the components. Although in that window there are a range of stoichiometries difficult to understand directly, the window limits – roughly defined by the right lines corresponding to the ratios CHI/PEO 3:2, pAPS/PEO 2:3 and CHI/PEO 1:2, Fig. 1a – may be to some extent rationalized considering the functionality of both the donors and the chitosan molecule. Both PEO and pAPS have each, one Lewis basic site per unit, while in chitosan there are two sugar hydroxyl groups as acid sites and an amine group as a basic one available for intermolecular interactions either with the donors or among chitosan chains. Products in the upper part of the compatibility window in Fig. 1a (CHI/PEO ratio ca. 3:2) appear, however, to be strongly marked by the ability of chitosan to form aggregates. This tendency to self-aggregate is

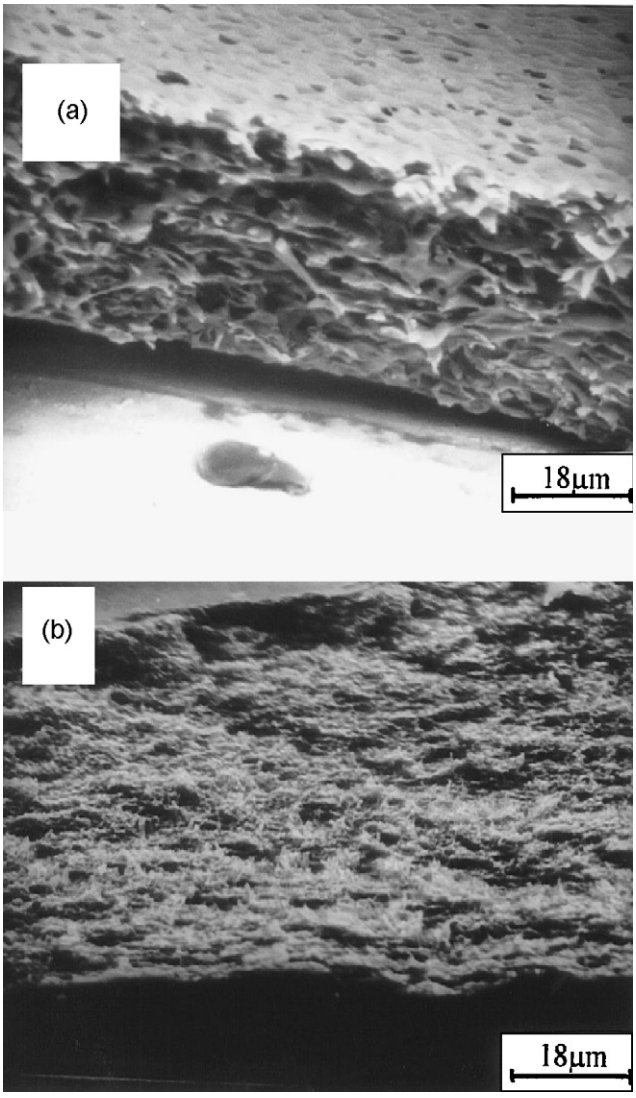

Fig. 4. SEM micrographs of the films: (a) POE/CHI/pAPS/Li^+ 1:0.5:0.6:0.2 and (b) POE/CHI/Li^+ 1:0.5:0.2.

indeed observed in pure chitosan [20] as well as in the molecular lamellar complexes CHI/pAPS [15] and in its composites with lithium salts [16,17] where, independent of the interactions with the silane, the polysaccharide is found forming domains which often show X-ray diffraction patterns similar to those of pure chitosan. Analogically, the molecular complexes along the CHI/PEO axe may be described as relatively rigid lamellae formed by chitosan chain aggregates flanked by the PEO strands held together by lithium ions located in the interlaminar spaces as a result of its stabilization by the polyether chains. The average composition of the films across the compatibility window goes from $Li_x(CHI)_1(PEO)_{0.6}$ to $Li_x(CHI)_1(PEO)_2(pAPS)_{1.2}$. In the ternary complexes, the donors pAPS and PEO would compete for both the coordination sites around these ions and for the acid sites on chitosan. However, given the relatively higher donor ability of the amine group, pAPS should be found preferentially around the lithium ions. Furthermore, since the molecular size of PEO is much higher than that of pAPS, a lamellar arrangement – constituted by a relatively rigid phase

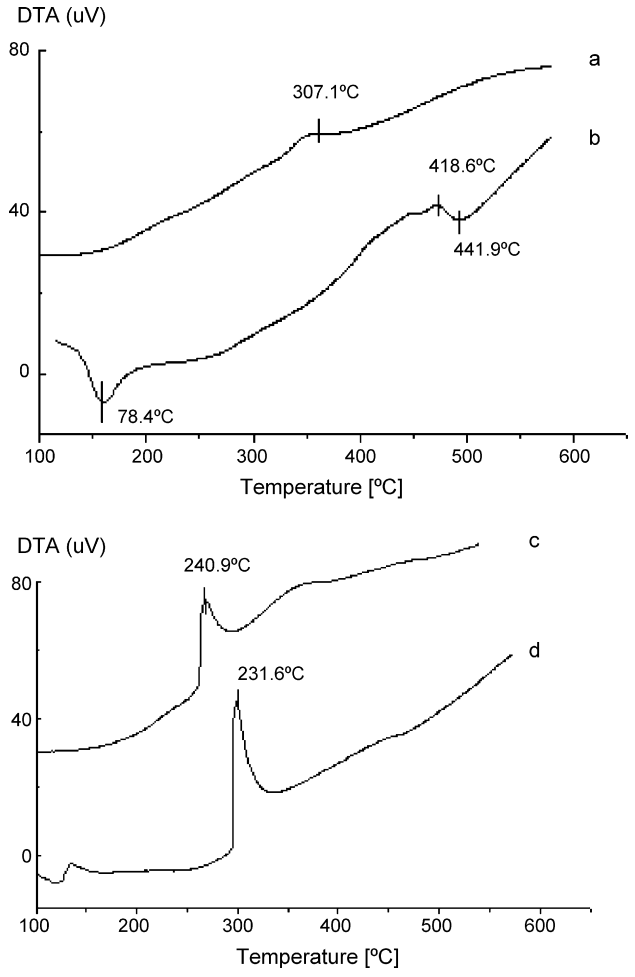

Fig. 5. DTA of the films: (a) chitosan (CHI); (b) poly(ethylene oxide) (POE); (c) POE/CHI/pAPS/Li^+ 1:0.5:0.6:0.2; (d) POE/CHI/Li^+ 1:0.5:0.2.

formed by chitosan and PEO and a somewhat mobile phase in which lithium ions are preferentially coordinated by pAPS – should be entropically more favorable. Preliminary experiments, analyzing ^{7}Li NMR selected samples [21], show that in these nanocomposites there is really a competition between PEO, CHI and pAPS for coordinating lithium. The same experiments also indicate the role of pAPS as both a plasticizer and a structural component.

The conductivity values observed for the composites agree with the model discussed above. Among the composites described here, the highest conductivity is observed for a complex near the CHI/PEO 1:2 limit, i.e. where the interface area is maximal. Conductivity also increases with the increasing exchange of the polyether by pAPS around lithium in the mobile phase. Thus, pAPS appears having an effect on the ionic conductivity like that of the plasticizer in the conventional PEO-based polymer electrolytes.

4. Conclusions

Because of its chemical functionality, one basic and two acidic sites per unit, chitosan frequently leads to hydrogen bonding self-aggregates. Notwithstanding that chitosan also interacts with other donor species for forming donor–acceptor macromolecular complexes within component concentration limits is strictly determined by the equivalency of the available sites. In our particular case, self-supported, molecularly compatible, lamellar CHI/PEO/pAPS nanocomposites containing a lithium salt are obtained by using stoichiometries in the range (3:2:0)–(1:2:1.4). The highest conductivity ca. 1.7×10^{-5} S cm^{-1} appears to be obtained when a structure constituted essentially by lithium ion coordinated by APS residues intercalated in a layered CHI/PEO matrix is formed. Given the observed conductivity, rather acceptable for a solid, as well as its high transparence, the product $(CHI)_1(PEO)_2(pAPS)_{1.2}$ described here is being evaluated as a material potentially useful for electroptical applications.

Acknowledgments

The authors thank the Universidad de Chile, the Universidad Católica del Norte and the FONDECYT (Grant 1050344) for partial financial support.

References

[1] F. Croce, L. Persi, F. Ronci, B. Scrosati, Solid State Ionics 315 (2000) 47.
[2] M.B. Armand, J.M. Chabagno, in: M.J. Duclot, P. Vishita, J.N. Mundoyand, G.K. Shenoy (Eds.), Fast Ion Transport in Solids, Elsevier, New York, 1979, p. 131.
[3] M. Armand, A. Gandini (Eds.), Third International Symposium on Polymer Electrolytes, Electrochim. Acta 37 (1992) 1469.
[4] E. Quartarone, C. Tomasi, A. Magistris, J. Thermal Anal. 46 (1996) 235.
[5] F. Serraino Fiory, F. Croce, A. D'Epifanio, S. Licoccia, B. Scrosati, E. Traversa, J. Eur. Ceram. Soc. 24 (2004) 1385.
[6] G. Appetecchi, Y. Aihara, B. Scrosati, Solid State Ionics 170 (2004) 63.
[7] B. Scrosati, C.A. Vincent, MRS Bull. 25 (2000) 28.
[8] J.K. Lee, Y.J. Lee, W.S. Chae, Y.M. Sung, J. Electroceram. 17 (2006) 941.
[9] Y.J. Wang, Y. Pam, D. Kim, Polym. Int. 56 (2007) 381.
[10] R.A. Muzarelli, Chitin, Pergamon Press, Oxford, 1977.
[11] H. Jiang, W. Su, S. Caracci, J. Appl. Polym. Sci. 61 (1996) 1163.
[12] B. Duan, C.H. Dong, X.Y. Yuan, K.D. Yao, J. Biomater. Sci.-Polym. 15 (2004) 797.
[13] N. Gorochovceva, R. Makuska, Eur. Polym. J. 40 (2004) 685.
[14] A. Nikolova, N. Manolova, I. Rashkov, Polym. Bull. 41 (1998) 115.
[15] S. Fuentes, P. Retuert, G. González, Int. J. Polym. Mater. 35 (1997) 61.
[16] S. Fuentes, P. Retuert, A. Ubilla, J. Fernández, G. González, Biomacromolecules 1 (2000) 239.
[17] S. Fuentes, P. Retuert, G. González, Electrochim. Acta 48 (2003) 2015.
[18] J.T.S. Irvine, D.R. Sinclair, A.R. West, Adv. Mater. 2 (1990) 132.
[19] A.K. Jonscher, Dielectric Relaxation in Solids, Chelsea Dielectrics Press, London, 1983.
[20] T. Rathke, S. Hudson, Rev. Macromol. Chem. Phys. C34 (1994) 375.
[21] J.P. Donoso, L.V.S. Lopes, A. Pawlicka, S. Fuentes, P.J. Retuert, G. González, Electrochim. Acta 53 (2007) 1455.